Electronic Supplementary Material (ESI) for CrystEngComm.

Supporting Information

Constructing pyrene-based dimer in a crystal by adjusting steric hindrance over the pyrene plane

Zhou-An Xia,[a‡] Xiangyu Zhang,[a‡] Chang Xi,[a] Qing Bai,[b] Haichao Liu,*[a] Shi-Tong Zhang,[a] and Bing Yang*[a]

[a] State Key Laboratory of Supramolecular Structure and Materials, College of Chemistry, Jilin University, Changchun, 130012, P. R. China

[b] College of New Materials and New Energies, Shenzhen Technology University, Shenzhen, 518118, P. R. China

Corresponding author e-mails: hcliu@jlu.edu.cn; yangbing@jlu.edu.cn

‡ These authors contributed equally.

SI Experimental details

SI-1 General information: All the reagents and solvents used for the synthesis were purchased from Aldrich and Acros companies and used without further purification. ^{1}H and ^{13}C NMR spectra were recorded on a Bruker AVANCE 500 spectrometer, using tetramethylsilane (TMS) as the internal standard. The mass spectra were recorded using a Thermo Fisher ITQ1100 instrument. Elementar vario MICRO cube Elemental Analyzer was used to perform the elemental analysis.

SI-2 Single crystal X-ray diffraction (SCXRD) data: The crystals of **Py-*o*BZT**, **Py-*m*BZT**, and **Py-*p*BZT** were obtained through solvent diffusion method in a system of tetrahydrofuran and methanol. The diffraction experiments were carried out on a Rigaku R-AXIS RAPID diffractometer equipped with a Mo-Kα (λ = 0.71073 Å) and control Software using the RAPID AUTO at room temperature. The crystal structures were solved with direct methods and refined with a full-matrix least-squares technique using the Olex2 programs. The non-hydrogen atoms were refined with anisotropic thermal parameters. Hydrogen atoms were set as riding on the parent atoms after placing them in idealized positions around respective parent atoms. Drawings of molecular conformations and molecular stacking structures were made using Mercury software.

SI-3 Photophysical measurements: UV-vis spectra of solutions were recorded on a Shimadzu UV-3100 Spectrophotometer. Emission spectra and time-resolved emission spectra were carried out on a FLS980 Spectrofluorometer. Photoluminescence quantum yields (PLQYs) were measured using an integrating sphere apparatus on a FLS980 Spectrofluorometer.

SI-4 Theoretical calculation: All the density functional theory (DFT) calculations were carried out using Gaussian 09 (version D.01) package on a PowerLeader cluster.[1] The optimization of ground state geometries of single molecules was carried out at the level of B3LYP /6-31G(d, p). The time-dependent density functional theory (TD-DFT) was carried out for the excited state geometry optimization at the level of M06-2X/6-31G(d, p), and the vertical excitation energies was calculated at the level of M06-2X/6-31G(d, p). Electrostatic potential (ESP) maps were obtained using an Multiwfn software and a VMD software.[2] Visualization analysis of weak interactions was made using an Multiwfn software and a VMD software. Interaction energy was calculated using a Multiwfn software based on AMBER forcefield, and the geometries used were directly taked out from the crystal structures. Two-dimonsional potential energy surface (PES) was simulated using

Gaussian 09 (version D.01) package combined with the Multiwfn software and Molclus software.[3] Specifically, the dimer structures with constant π–π distance (3.5 Å) and different π–π overlap (step length is 0.1 Å) were constructed through the coordinate transformation function of Multiwfn software, and the π–π distance of 3.5 Å was used on basis of the analysis of the actual geometry of the pyrene dimer in crystal packing structures. The xyz2QC subroutine of Molclus software was used to construct the input documents for Gaussian calculation.

SII Synthetic details

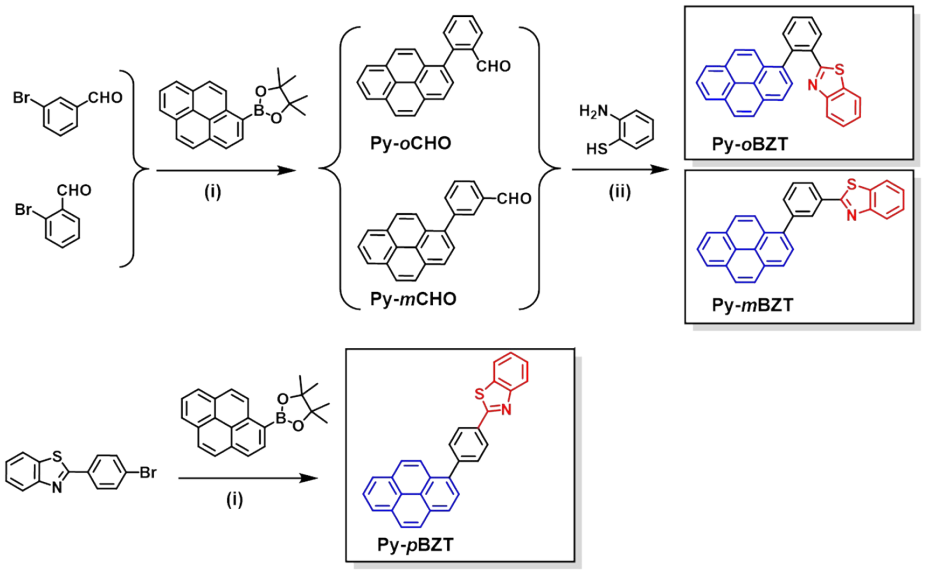

Scheme S1. Synthetic routes to **Py-*o*BZT**, **Py-*m*BZT**, and **Py-*p*BZT** compounds. (i) K_2CO_3, $Pd(PPh_3)_4$, H_2O, toluene, 90 ℃ for 48 h in nitrogen (N_2) atmosphere; (ii) DMSO, 170 ℃ for 12 h.

Synthesis of 2-(2-(pyren-1-yl)phenyl)benzo[*d*]thiazole (Py-*o*BZT)

A mixture of 4,4,5,5-tetramethyl-2-(pyren-1-yl)-1,3,2-dioxaborolane (820 mg, 2.50 mmol), 2-bromobenzaldehyde (460 mg, 2.50 mmol), K_2CO_3 (3.46 g, 25.00 mmol), distilled water (15 mL), and toluene (30 mL) was degassed and recharged with nitrogen. Then $Pd(PPh_3)_4$ (92 mg, 0.08 mmol) was added in the mixture as catalyst and the mixture was degassed and recharged with nitrogen again. After stirred and heated under reflux at 90 ℃ for 48 h, the cooled reaction mixture was extracted with dichloromethane. The organic phase was filtered and concentrated in a vacuum. It was purified via silica gel chromatography by petroleum ether and dichloromethane to afford pale yellow solid **Py-*o*CHO** in 53% yield (405 mg). ^{1}H NMR (500 MHz, DMSO-d_6, TMS, 25 ℃): δ= 9.59 (s, 1H), 8.41 (dd, J = 17.6, 7.7 Hz, 2H), 8.33 (d, J = 7.6 Hz, 1H), 8.30 (s, 2H), 8.21 – 8.04 (m, 4H), 7.92 (td, J = 7.5, 1.4 Hz, 1H), 7.78 (t, J = 7.6 Hz, 1H), 7.68 (dd, J = 17.1, 8.3 Hz, 2H).

A mixture of **Py-*o*CHO** (397 mg, 1.30 mmol) and 2-aminobenzenethiol (195 mg, 1.56 mmol) in DMSO (20 mL) was stirred under nitrogen atmosphere for 12 h at 170 ℃. The reaction was then stopped, most of the DMSO was evaporated under reduced pressure, and the crude was purified via silica gel chromatography by petroleum ether and dichloromethane to afford the yellow powder **Py-**

***o*BZT** in 63% yield (337 mg). ^{1}H NMR (500 MHz, DMSO-d_6, TMS, 25 ℃): δ= 8.49 – 8.43 (m, 1H), 8.40 (d, J = 7.8 Hz, 1H), 8.36 (d, J = 7.0 Hz, 1H), 8.30 (d, J = 9.3 Hz, 2H), 8.25 (d, J = 7.3 Hz, 1H), 8.09 (dt, J = 11.8, 8.0 Hz, 2H), 8.04 (d, J = 7.8 Hz, 1H), 7.94 (d, J = 8.1 Hz, 1H), 7.80 – 7.75 (m, 2H), 7.70 (d, J = 9.2 Hz, 1H), 7.63 – 7.57 (m, 2H), 7.41 – 7.35 (m, 1H), 7.21 – 7.15 (m, 1H). ^{13}C NMR (126 MHz, $CDCl_3$, TMS, 25℃): δ= 167.20, 151.58, 140.30, 136.15, 135.04, 133.51, 132.33 (CH), 131.54, 131.38, 130.96, 130.25 (CH), 130.08 (CH), 128.48 (CH), 128.40 (CH), 128.12 (CH), 127.93 (CH), 127.51 (CH), 126.17 (CH), 125.95 (CH), 125.41 (CH), 125.35 (CH), 124.82 (CH), 122.81 (CH), 121.23 (CH). GC/MS, EI (mass m/z): 411.84 [M^+] (calcd: 411.52). Anal. Calcd for $C_{29}H_{17}NS$: C, 84.64; H, 4.16; N, 3.40; S, 7.79. Found: C, 85.24; H, 4.16; N, 3.40; S, 8.08.

Synthesis of 2-(3-(pyren-1-yl)phenyl)benzo[*d*]thiazole (Py-*m*BZT)

A mixture of 4,4,5,5-tetramethyl-2-(pyren-1-yl)-1,3,2-dioxaborolane (820 mg, 2.50 mmol), 3-bromobenzaldehyde (460 mg, 2.50 mmol), K_2CO_3 (3.46 g, 25.00 mmol), distilled water (15 mL), and toluene (30 mL) was degassed and recharged with nitrogen. Then $Pd(PPh_3)_4$ (92 mg, 0.08 mmol) was added in the mixture as catalyst and the mixture was degassed and recharged with nitrogen again. After stirred and heated under reflux at 90 ℃ for 48 h, the cooled reaction mixture was extracted with dichloromethane. The organic phase was filtered and concentrated in a vacuum. It was purified via silica gel chromatography by petroleum ether and dichloromethane to afford white solid **Py-*m*CHO** in 83% yield (643 mg). ^{1}H NMR (500 MHz, DMSO-d_6, TMS, 25 ℃): δ= 10.19 (s, 1H), 8.43 (d, J = 7.8 Hz, 1H), 8.37 (d, J = 7.6 Hz, 1H), 8.33 (d, J = 7.6 Hz, 1H), 8.28 (s, 2H), 8.22 (d, J = 9.2 Hz, 1H), 8.18 (d, J = 1.9 Hz, 1H), 8.12 – 8.07 (m, 4H), 8.01 (d, J = 7.5 Hz, 1H), 7.87 (t, J = 7.6 Hz, 1H).

A mixture of **Py-*m*CHO** (635 mg, 2.07 mmol) and 2-aminobenzenethiol (310 mg, 2.48 mmol) in DMSO (25 mL) was stirred under nitrogen atmosphere for 12 h at 170 ℃. The reaction was then stopped, most of the DMSO was evaporated under reduced pressure, and the crude was purified via silica gel chromatography by petroleum ether and dichloromethane to afford the brownish yellow powder **Py-*m*BZT** in 77% yield (655 mg). ^{1}H NMR (400 MHz, DMSO-d_6, TMS, 25℃): δ= 8.46 (d, J = 7.8 Hz, 1H), 8.39 (d, J = 7.6 Hz, 1H), 8.35 (t, J = 3.8 Hz, 2H), 8.31 – 8.09 (m, 9H), 7.91 – 7.83 (m, 2H), 7.59 (t, J = 7.6 Hz, 1H), 7.51 (t, J = 7.6 Hz, 1H). ^{13}C NMR (126 MHz, $CDCl_3$, TMS, 25 ℃): δ=168.02, 153.94, 142.24, 136.55, 135.03, 133.76, 133.27 (CH), 131.50, 130.96, 129.63

(CH), 129.12 (CH), 128.58, 127.87 (CH), 127.68 (CH), 127.58 (CH), 127.43 (CH), 126.49 (CH), 126.13 (CH), 125.38 (CH), 125.32 (CH), 125.04 (CH), 124.94 (CH), 124.88, 124.72 (CH), 123.28 (CH), 121.69 (CH). GC/MS, EI (mass m/z): 411.00 [M^+] (calcd: 411.52). Anal. Calcd for $C_{29}H_{17}NS$: C, 84.64; H, 4.16; N, 3.40; S, 7.79. Found: C, 85.03; H, 4.13; N, 3.48; S, 7.94.

2-(4-(pyren-1-yl)phenyl)benzo[*d*]thiazole (Py-*p*BZT)

A mixture of 4,4,5,5-tetramethyl-2-(pyren-1-yl)-1,3,2-dioxaborolane (820 mg, 2.50 mmol), 2-(4-bromophenyl)benzo[*d*]thiazole (727 mg, 2.50 mmol), K_2CO_3 (3.46 g, 25.00 mmol), distilled water (15 mL), and toluene (30 mL) was degassed and recharged with nitrogen. Then $Pd(PPh_3)_4$ (92 mg, 0.08 mmol) was added in the mixture as catalyst and the mixture was degassed and recharged with nitrogen again. After stirred and heated under reflux at 90 ℃ for 48 h, the cooled reaction mixture was extracted with dichloromethane. The organic phase was filtered and concentrated in a vacuum. It was purified via silica gel chromatography by petroleum ether and dichloromethane to afford white solid **Py-*p*BZT** in 83% yield (855 mg). ^{1}H NMR (500 MHz, DMSO-d_6, TMS, 25 ℃): δ= 8.43 (d, J = 7.8 Hz, 1H), 8.36 (q, J = 8.0 Hz, 4H), 8.28 (s, 2H), 8.26 – 8.18 (m, 3H), 8.14 (t, J = 7.9 Hz, 3H), 7.88 (d, J = 8.1 Hz, 2H), 7.61 (t, J = 7.7 Hz, 1H), 7.53 (t, J = 7.6 Hz, 1H). ^{13}C NMR (126 MHz, $CDCl_3$, TMS, 25℃): δ= 167.92, 153.94, 144.24, 136.52, 134.99, 132.34, 131.49, 131.32 (CH), 131.00, 128.46, 127.89 (CH), 127.76 (CH), 127.70 (CH), 127.40 (CH), 126.54 (CH), 126.16 (CH), 125.38 (CH), 125.07 (CH), 124.92 (CH), 124.75 (CH), 123.23 (CH), 121.72 (CH). GC/MS, EI (mass m/z): 411.11 [M^+] (calcd: 411.52). Anal. Calcd for $C_{29}H_{17}NS$: C, 84.64; H, 4.16; N, 3.40; S, 7.79. Found: C, 85.12; H, 4.16; N, 3.44; S, 7.97.

SIII Figures and tables

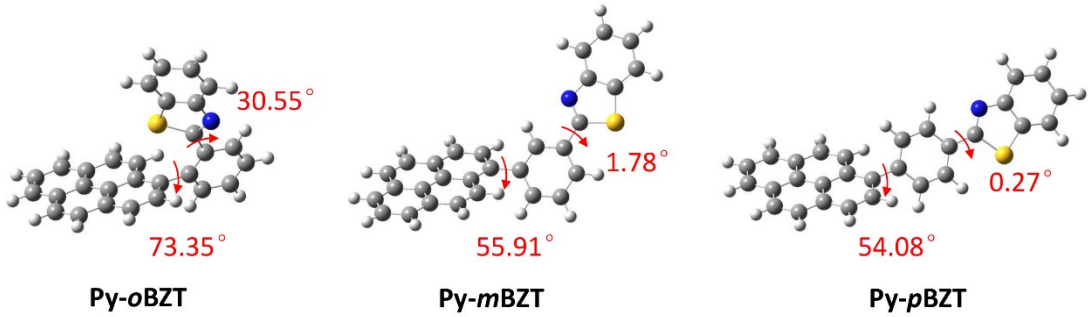

Figure S1. Optimized ground state geometries of **Py-*o*BZT**, **Py-*m*BZT**, and **Py-*p*BZT**.

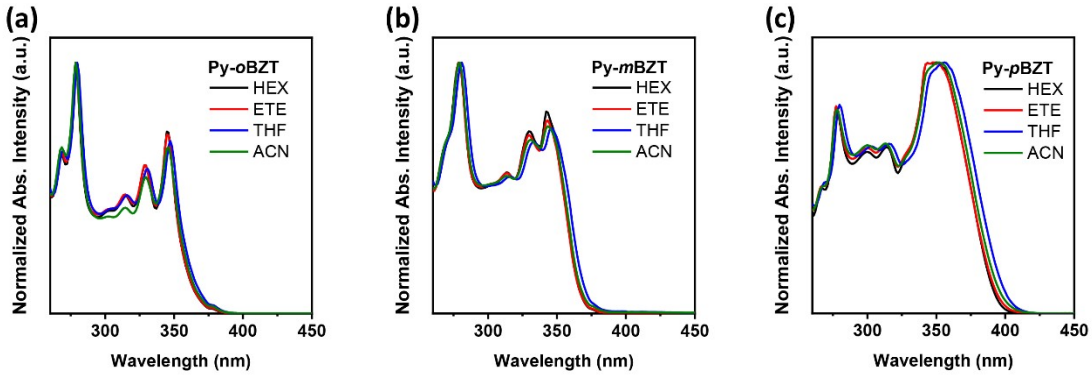

Figure S2. Absorption spectra of (a) **Py-*o*BZT**, (b) **Py-*m*BZT**, and (c) **Py-*p*BZT** diluted in solvents with different polarities. Concentration is controlled to be 10 μM. HEX is hexane, ETE is ethyl ether, THF is tetrahydrofuran, and ACN is acetonitrile.

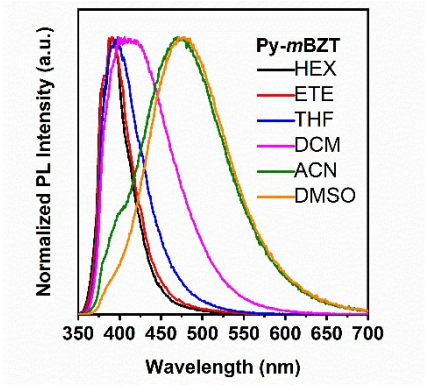

Figure S3. Emission spectra of **Py-*m*BZT** diluted in solvents with different polarities. Concentration is controlled to be 10 μM. HEX is hexane, ETE is ethyl ether, THF is tetrahydrofuran, DCM is dichloromethane, ACN is acetonitrile, and DMSO is dimethyl sulfoxide.

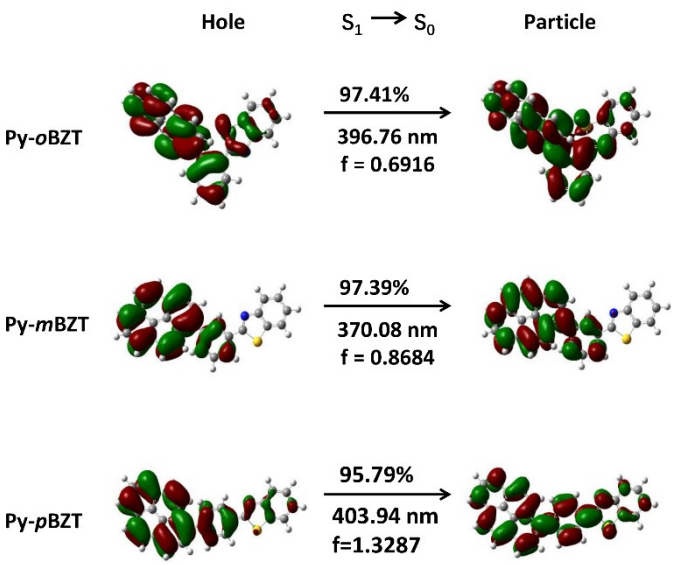

Figure S4. NTOs of S_1 state of **Py-*o*BZT**, **Py-*m*BZT**, and **Py-*p*BZT**.

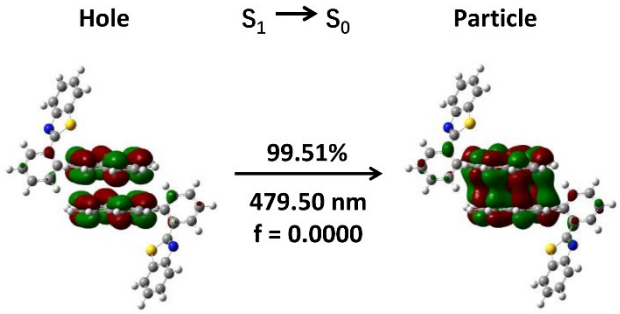

Figure S5. NTOs of S_1 state of the pyrene-based dimer for **Py-*o*BZT**.

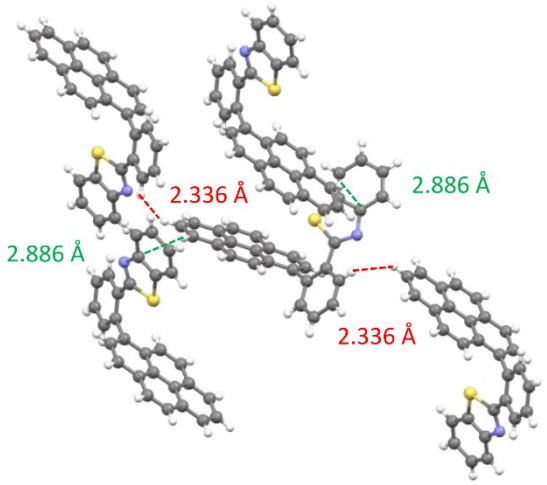

Figure S6. Intermolecular interactions in the **Py-*o*BZT** crystal.

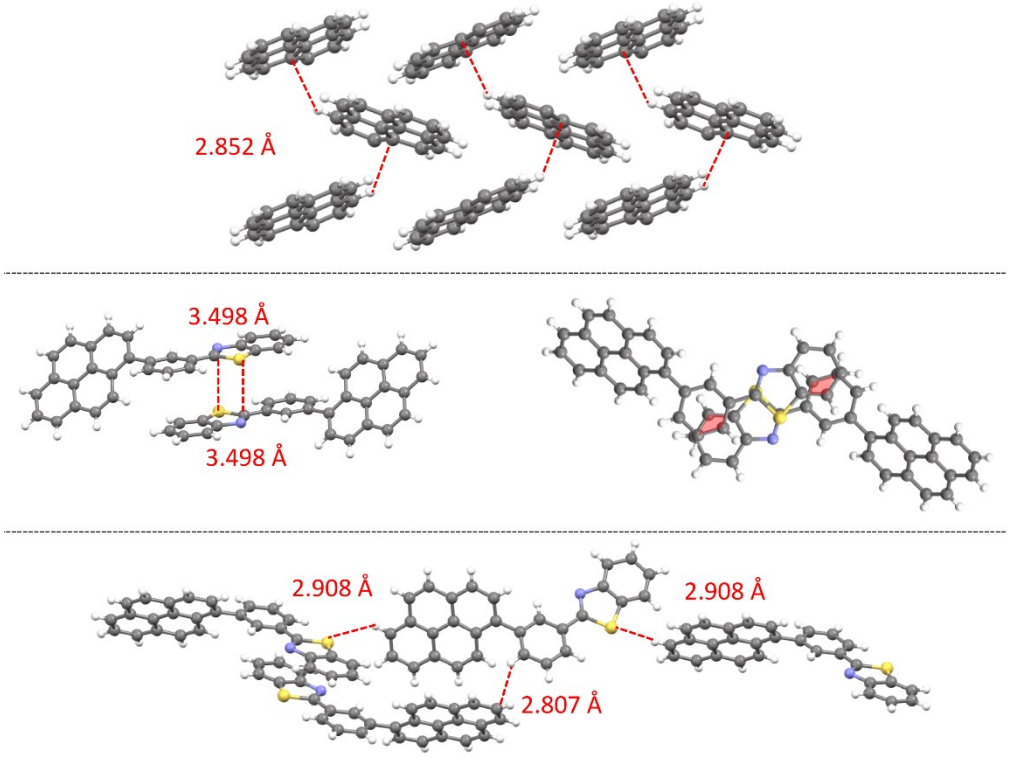

Figure S7. Intermolecular interactions in the **Py-*m*BZT** crystal.

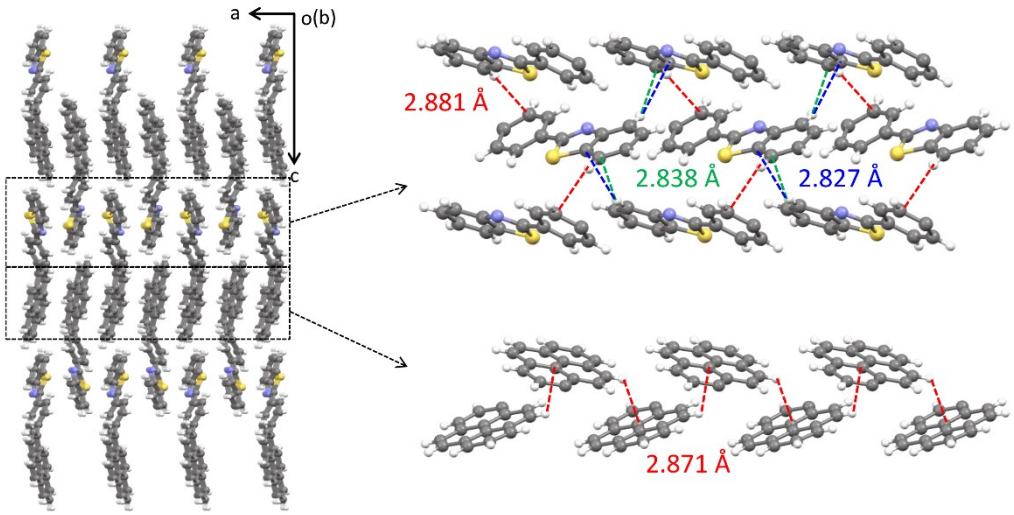

Figure S8. Intermolecular interactions in the **Py-*p*BZT** crystal.

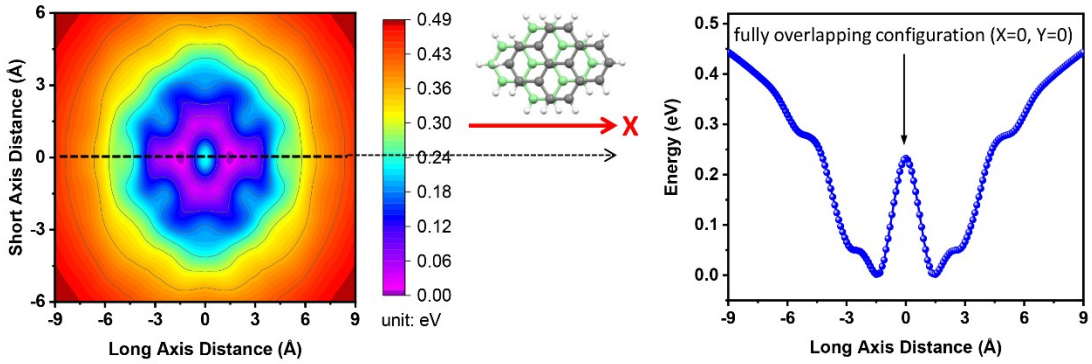

Figure S9. Simulation of the PES of the pyrene dimer in its ground state (S_0) geometry. The X and Y parameters refer to the translational shift of the center-of-mass of the two pyrene molecules along the long axis and short axis of pyrene molecule, respectively. It is assumed that the pyrene molecular plane is strictly normal to the Z-axis.

For example, we plot a one-dimensional potential energy curve against variable X coordinate when Y=0. Observed from **Figure S9**, a local maximum was found at the fully overlapping configuration, that is, (X=0, Y=0). Moreover, when two pyrene molecules slip along the X direction (long axis of pyrene), they go through multiple maxima/minima points.

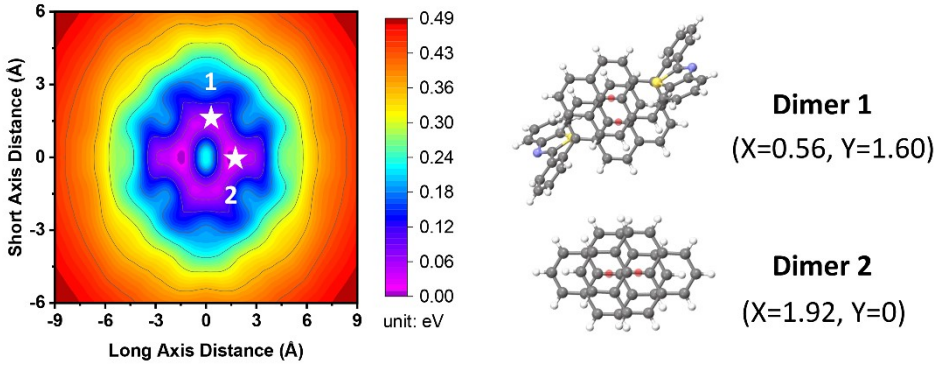

Figure S10. Simulation of the PES of the pyrene dimer in its ground state (S_0) geometry on the left, and molecular orientation of dimer 1 (pyrene-based dimer for Py-*o*BZT) and dimer 2 (pyrene dimer) on the right. Red ball represents the center-of-mass of each pyrene molecule.

The potential energy actually changed little as a function of π–π distance, as verified in our previous paper.[4] Therefore in this work, we focus on the potential energy as a function of X and Y variables, that is, potential energy against overlap ratio. After calculation on X and Y slippage, dimer 1 and dimer 2 occupy different potential wells as dictated by the two-dimensional PES.

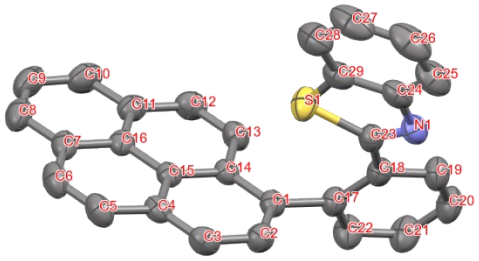

Figure S11. Representative ortep diagram of **Py-*o*BZT**. Thermal ellipsoids are set at 50% probability level. All the hydrogen atoms are omitted for clarity.

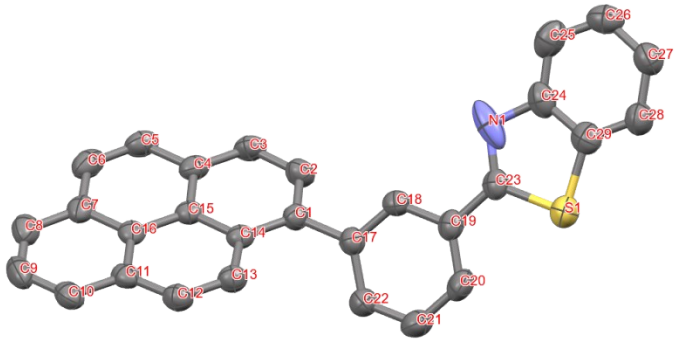

Figure S12. Representative ortep diagram of **Py-*m*BZT**. Thermal ellipsoids are set at 50% probability level. All the hydrogen atoms are omitted for clarity.

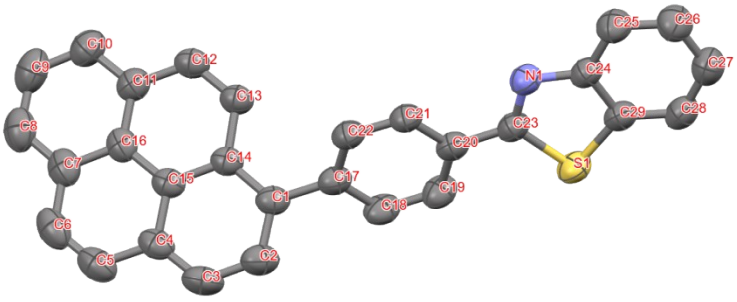

Figure S13. Representative ortep diagram of **Py-*p*BZT**. Thermal ellipsoids are set at 50% probability level. All the hydrogen atoms are omitted for clarity.

Table S1. Crystallographic data of **Py-*o*BZT**, **Py-*m*BZT**, and **Py-*p*BZT** compounds.

compound	**Py-*o*BZT**	**Py-*m*BZT**	**Py-*p*BZT**
crystal color	colorless	colorless	colorless
empirical formula	$C_{29}H_{17}NS$	$C_{29}H_{17}NS$	$C_{29}H_{17}NS$
formula weight	411.49	411.49	411.49
T [K]	293.0	293.0	294.0
crystal system	monoclinic	orthorhombic	orthorhombic
space group	$P2_1/c$	Pbca	$P2_12_12_1$
a [Å]	13.1520(5)	15.7355(6)	7.7310(6)
b [Å]	14.0836(5)	8.0029(3)	8.1036(5)
c [Å]	12.0152(5)	31.7701(13)	32.103(2)
α [°]	90	90	90
β [°]	115.0090	90	90
γ [°]	90	90	90
V [Å^3]	2016.88(14)	4000.8(3)	2011.2(2)
Z	4	8	4
F(000)	856.0	1712.0	856.0
density [g·cm^{-3}]	1.355	1.366	1.359
μ [mm^{-1}]	0.178	0.179	0.178
reflections collected	52745	146830	46705
unique reflections	4619	4072	4282
R (int)	0.0399	0.1529	0.0873
GOF	1.063	0.891	1.085
R_1 [I>2σ(I)]	0.0427	0.0904	0.0421
ωR_2 [I>2σ(I)]	0.1018	0.2221	0.0840
R_1 (all data)	0.0596	0.1263	0.0911
ωR_2 (all data)	0.1161	0.2562	0,1063
CCDC number	2284247	2284246	2284248

Table S2. Bond lengths (Å) for **Py-*o*BZT**.

Atom	Atom	Length/Å	Atom	Atom	Length/Å
S1	C23	1.7582(16)	C16	C11	1.417(2)
S1	C29	1.7289(18)	C16	C7	1.425(2)
N1	C23	1.295(2)	C13	C12	1.351(2)
N1	C24	1.385(2)	C29	C28	1.394(3)
C15	C14	1.425(2)	C11	C12	1.430(2)
C15	C4	1.420(2)	C11	C10	1.400(2)
C15	C16	1.421(2)	C2	C3	1.379(2)
C14	C1	1.407(2)	C7	C6	1.432(3)
C14	C13	1.436(2)	C7	C8	1.392(3)
C18	C23	1.478(2)	C5	C6	1.333(3)
C18	C17	1.403(2)	C19	C20	1.379(2)
C18	C19	1.401(2)	C20	C21	1.377(3)
C1	C17	1.492(2)	C22	C21	1.379(2)
C1	C2	1.391(2)	C28	C27	1.383(3)
C4	C3	1.389(2)	C10	C9	1.383(3)
C4	C5	1.436(2)	C8	C9	1.369(3)
C24	C29	1.396(3)	C25	C26	1.372(3)
C24	C25	1.393(3)	C27	C26	1.388(4)
C17	C22	1.394(2)			

Table S3. Bond Angles for **Py-*o*BZT**.

Atom	Atom	Atom	Angle/°	Atom	Atom	Atom	Angle/°
C29	S1	C23	89.17(8)	C11	C16	C7	119.74(15)
C23	N1	C24	111.24(14)	C12	C13	C14	121.45(15)
C4	C15	C14	120.00(14)	C24	C29	S1	109.42(12)
C4	C15	C16	119.86(14)	C28	C29	S1	129.24(16)
C16	C15	C14	120.15(14)	C28	C28	C24	121.33(18)
C15	C14	C13	118.03(14)	C16	C11	C12	118.24(15)
C1	C14	C15	119.02(14)	C10	C11	C16	118.94(17)
C1	C14	C13	122.94(14)	C10	C11	C12	122.82(17)
C17	C18	C23	124.34(14)	C3	C2	C1	121.52(15)
C19	C18	C23	116.77(14)	C16	C7	C6	118.40(16)
C19	C18	C17	118.89(15)	C8	C7	C16	118.62(18)
C14	C1	C17	121.38(14)	C8	C7	C6	122.97(17)
C2	C1	C14	119.61(14)	C2	C3	C4	120.79(15)
C2	C1	C17	119.01(14)	C6	C5	C4	121.53(17)
N1	C23	S1	115.01(12)	C20	C19	C18	121.18(16)
N1	C23	C18	121.45(14)	C13	C12	C11	121.76(15)
C18	C23	S1	123.47(12)	C21	C20	C19	119.86(16)
C15	C4	C5	118.55(16)	C5	C26	C7	121.76(15)
C3	C4	C15	119.03(14)	C21	C22	C17	121.64(17)
C3	C4	C5	122.42(15)	C20	C21	C22	119.77(17)
N1	C24	C29	115.14(15)	C27	C28	C29	117.8(2)
N1	C24	C25	125.16(18)	C9	C10	C11	120.5(2)
C25	C24	C29	119.69(18)	C9	C8	C7	121.34(18)
C18	C17	C1	122.19(14)	C8	C9	C10	120.80(18)
C22	C17	C18	118.64(15)	C26	C25	C24	119.0(2)
C22	C17	C1	119.12(15)	C28	C27	C26	121.1(2)

C15	C16	C7	119.89(15)	C25	C26	C27	121.2(2)
C11	C16	C15	120.37(14)				

Table S4. Bond lengths (Å) for **Py-*m*BZT**.

Atom	Atom	Length/Å	Atom	Atom	Length/Å
S1	C23	1.779(4)	C7	C8	1.397(6)
S1	C29	1.753(5)	C19	C18	1.401(6)
N1	C23	1.358(7)	C19	C20	1.373(6)
N1	C24	1.413(6)	C17	C18	1.395(6)
C14	C15	1.425(5)	C17	C22	1.406(6)
C14	C1	1.404(6)	C13	C12	1.357(6)
C14	C13	1.432(5)	C28	C29	1.361(6)
C15	C16	1.433(5)	C28	C27	1.376(7)
C15	C4	1.420(6)	C3	C2	1.385(6)
C16	C11	1.419(6)	C6	C5	1.347(7)
C16	C7	1.412(6)	C24	C29	1.373(7)
C1	C17	1.494(5)	C24	C25	1.392(7)
C1	C2	1.390(6)	C22	C21	1.381(6)
C11	C12	1.423(6)	C10	C9	1.376(7)
C11	C10	1.400(6)	C27	C26	1.366(7)
C4	C3	1.388(6)	C21	C20	1.390(7)
C4	C5	1.440(6)	C9	C8	1.374(7)
C23	C19	1.445(6)	C26	C25	1.418(8)
C7	C6	1.433(7)			

Table S5. Bond Angles for **Py-*m*BZT**.

Atom	Atom	Atom	Angle/°	Atom	Atom	Atom	Angle/°
C29	S1	C23	87.9(2)	C20	C19	C18	119.6(4)
C23	N1	C24	107.2(5)	C18	C17	C1	120.2(4)
C15	C14	C13	118.1(4)	C18	C17	C22	118.4(4)
C1	C14	C15	118.2(3)	C22	C17	C1	121.4(4)
C1	C14	C13	123.6(4)	C17	C18	C19	121.0(4)
C14	C15	C16	120.0(3)	C12	C13	C14	121.5(4)
C4	C15	C14	120.0(3)	C13	C12	C11	121.8(4)
C4	C15	C16	119.3(4)	C29	C28	C27	119.7(5)
C11	C16	C15	119.9(4)	C2	C3	C4	120.8(4)
C7	C16	C15	120.1(4)	C3	C2	C1	121.1(4)
C7	C16	C11	120.0(4)	C5	C6	C7	121.7(4)
C14	C1	C17	122.4(3)	C29	C24	N1	117.7(5)
C2	C1	C14	120.3(4)	C29	C24	C25	119.9(4)
C2	C1	C17	117.3(4)	C25	C24	N1	122.4(5)
C16	C11	C12	118.6(4)	C6	C5	C4	120.7(4)
C10	C11	C16	118.4(4)	C21	C22	C17	120.2(4)
C10	C11	C12	123.0(4)	C9	C10	C11	121.3(5)
C15	C4	C5	119.3(4)	C28	C29	S1	127.0(4)
C3	C4	C15	118.7(4)	C28	C29	C24	122.3(5)
C3	C4	C5	122.0(4)	C24	C29	S1	110.7(4)
N1	C23	S1	116.5(3)	C26	C27	C28	120.9(5)
N1	C23	C19	123.4(4)	C22	C21	C20	120.7(4)
C19	C23	S1	120.0(3)	C19	C20	C21	120.2(4)
C16	C7	C6	118.9(4)	C8	C9	C10	120.1(4)
C8	C7	C16	118.8(4)	C27	C26	C25	120.6(5)
C8	C7	C6	122.3(4)	C9	C8	C7	121.3(5)

C18	C19	C23	119.6(4)	C24	C25	C26	117.5(4)
C20	C19	C23	120.8(4)				

Table S6. Bond lengths (Å) for **Py-*p*BZT**.

Atom	Atom	Length/Å	Atom	Atom	Length/Å
S1	C23	1.751(3)	C17	C18	1.402(5)
S1	C29	1.729(4)	C13	C12	1.353(5)
N1	C23	1.297(5)	C11	C12	1.424(5)
N1	C24	1.390(5)	C11	C10	1.397(5)
C21	C20	1.400(5)	C24	C25	1.388(5)
C21	C22	1.377(5)	C1	C2	1.395(5)
C20	C23	1.466(5)	C4	C3	1.388(5)
C20	C19	1.379(5)	C4	C5	1.431(5)
C15	C14	1.419(5)	C18	C19	1.380(5)
C15	C16	1.425(5)	C28	C27	1.369(5)
C15	C4	1.425(50	C2	C3	1.378(6)
C22	C17	1.391(5)	C25	C26	1.375(5)
C14	C13	1.439(5)	C7	C6	1.425(6)
C14	C1	1.412(5)	C7	C8	1.396(6)
C16	C11	1.415(5)	C10	C9	1.385(6)
C16	C7	1.417(5)	C6	C5	1.338(6)
C29	C24	1.400(5)	C27	C26	1.388(5)
C29	C28	1.388(5)	C8	C9	1.383(6)
C17	C1	1.485(5)			

Table S7. Bond Angles for **Py-*p*BZT**.

Atom	Atom	Atom	Angle/°	Atom	Atom	Atom	Angle/°
C29	S1	C23	89.32(18)	C10	C11	C12	121.9(4)
C23	N1	C24	110.3(3)	N1	C24	C29	115.6(3)
C22	C21	C20	120.5(3)	C25	C24	N1	124.7(3)
C21	C20	C23	119.1(3)	C25	C24	C29	119.6(4)
C19	CC20	C21	119.2(3)	C14	C1	C17	122.6(3)
C19	C20	C23	119.1(3)	C2	C1	C14	119.3(3)
C14	C15	C16	120.5(3)	C2	C1	C17	118.1(3)
C14	C15	C4	120.1(3)	C15	C4	C5	118.4(4)
C4	C15	C16	119.4(3)	C3	C4	C15	118.5(4)
N1	C23	S1	115.7(3)	C3	C4	C5	123.1(4)
N1	C23	C20	122.9(3)	C13	C12	C11	121.6(4)
C20	C23	S1	121.4(3)	C19	C18	C17	120.8(3)
C21	C22	C17	121.5(3)	C27	C28	C29	118.5(4)
C15	C14	C13	117.6(3)	C20	C19	C18	121.3(4)
C1	C14	C15	119.4(3)	C3	C2	C1	121.0(4)
C1	C14	C13	122.9(3)	C2	C3	C4	121.7(4)
C11	C16	C15	120.3(3)	C26	C25	C24	119.2(4)
C11	C16	C7	119.6(4)	C16	C7	C6	118.4(4)
C7	C16	C15	120.3(4)	C8	C7	C16	119.0(4)
C24	C29	S1	109.0(3)	C8	C7	C6	122.6(4)
C28	C29	S1	130.2(3)	C9	C10	C11	120.4(4)
C28	C29	C24	120.8(4)	C5	C6	C7	121.7(4)
C22	C17	C1	120.8(3)	C6	C5	C4	121.7(4)
C22	C17	C18	117.5(3)	C28	C27	C26	121.2(4)
C18	C17	C1	121.6(3)	C9	C8	C7	121.0(4)
C12	C13	C14	121.7(3)	C25	C26	C27	120.6(4)

C16	C11	C12	118.5(3)	C8	C9	C10	120.5(4)
C10	C11	C16	119.6(4)				

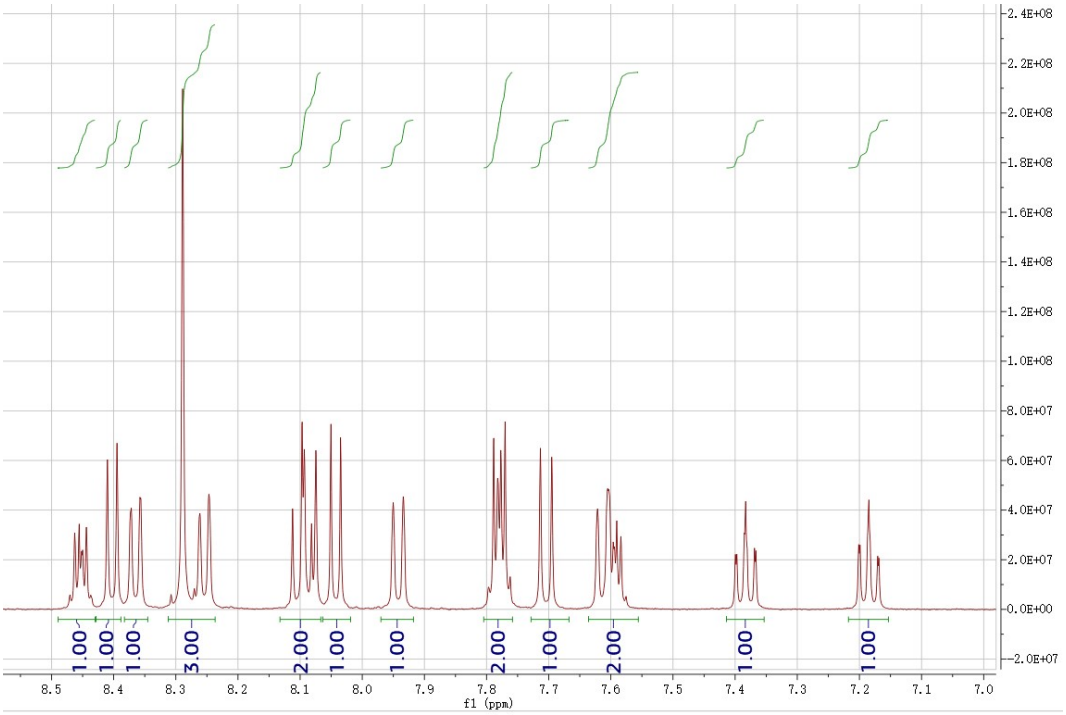

Figure S14. [1]H NMR spectrum of **Py-*o*BZT** compound.

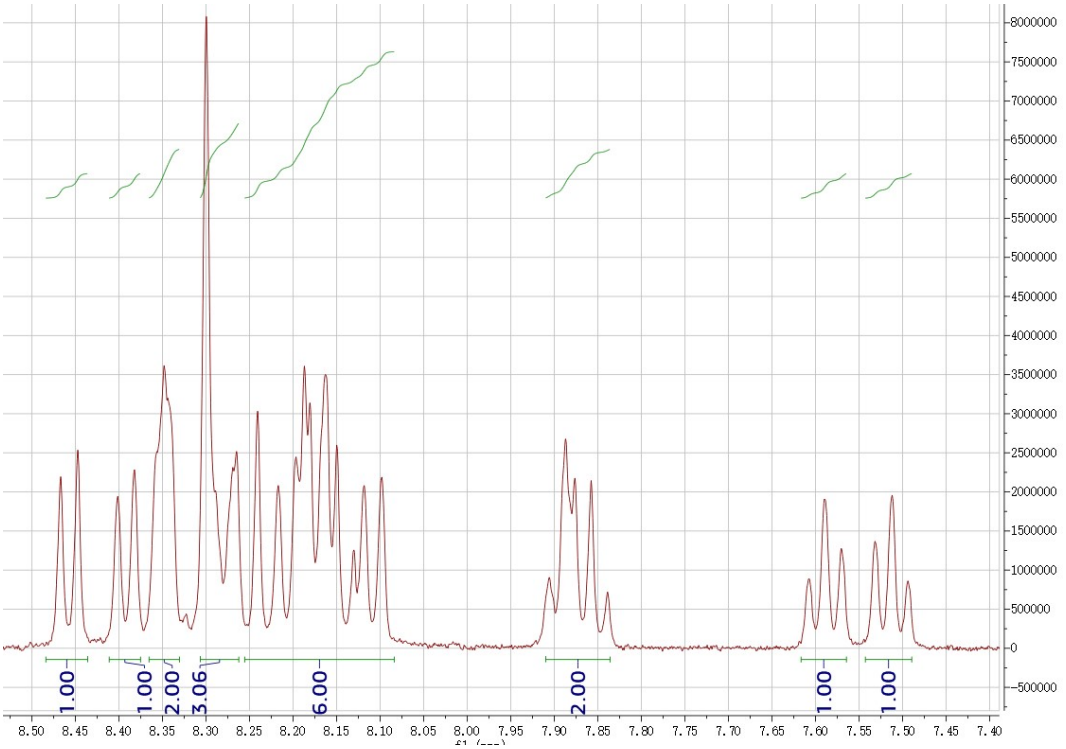

Figure S15. [1]H NMR spectrum of **Py-*m*BZT** compound.

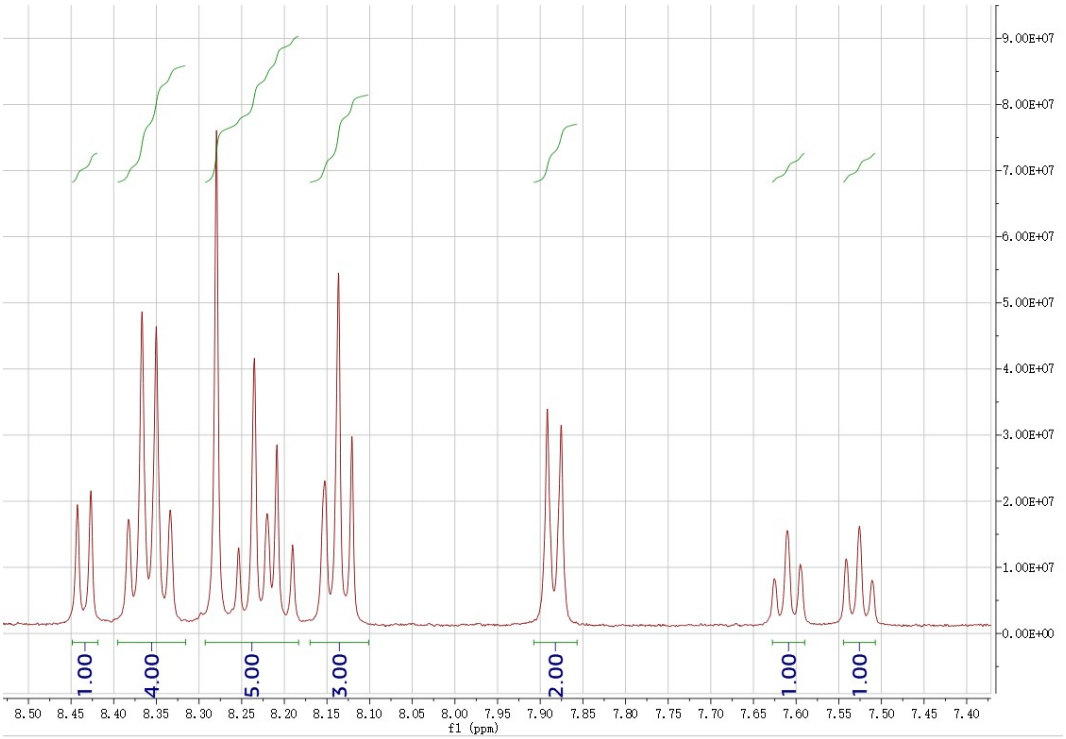

Figure S16. ^{1}H NMR spectrum of **Py-*p*BZT** compound.

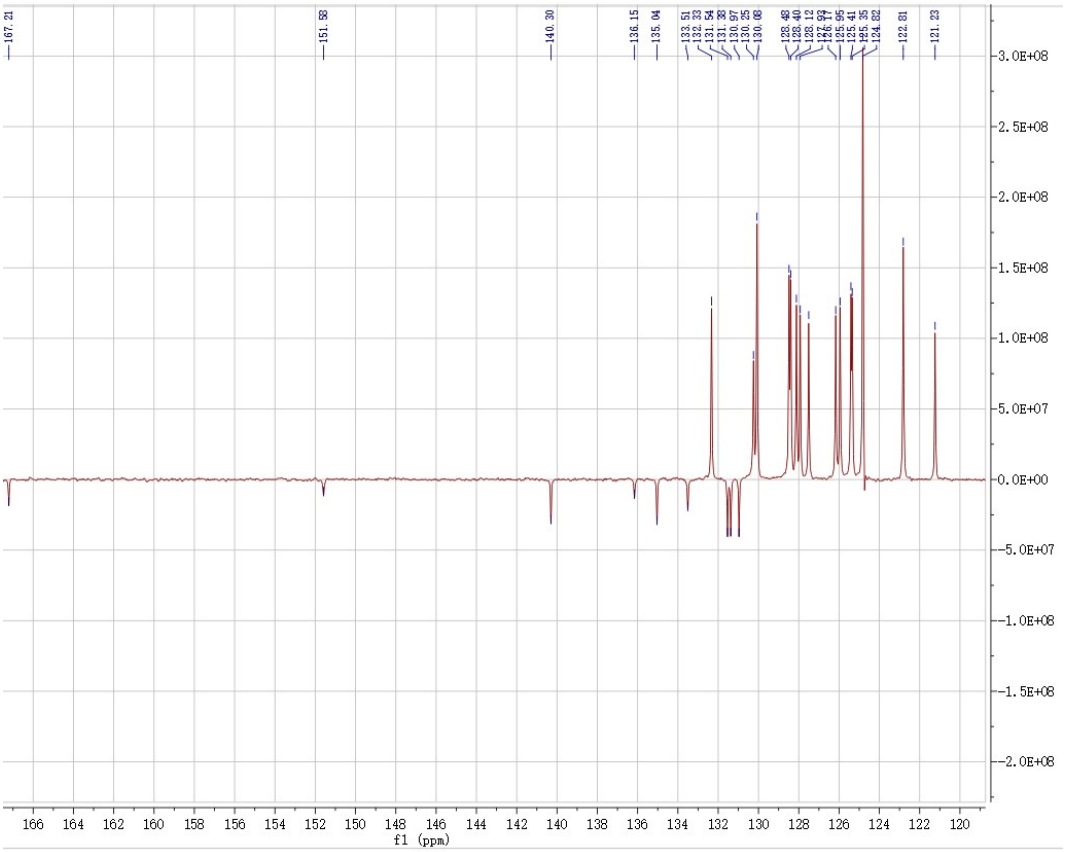

Figure S17. ^{13}C NMR spectrum of **Py-*o*BZT** compound.

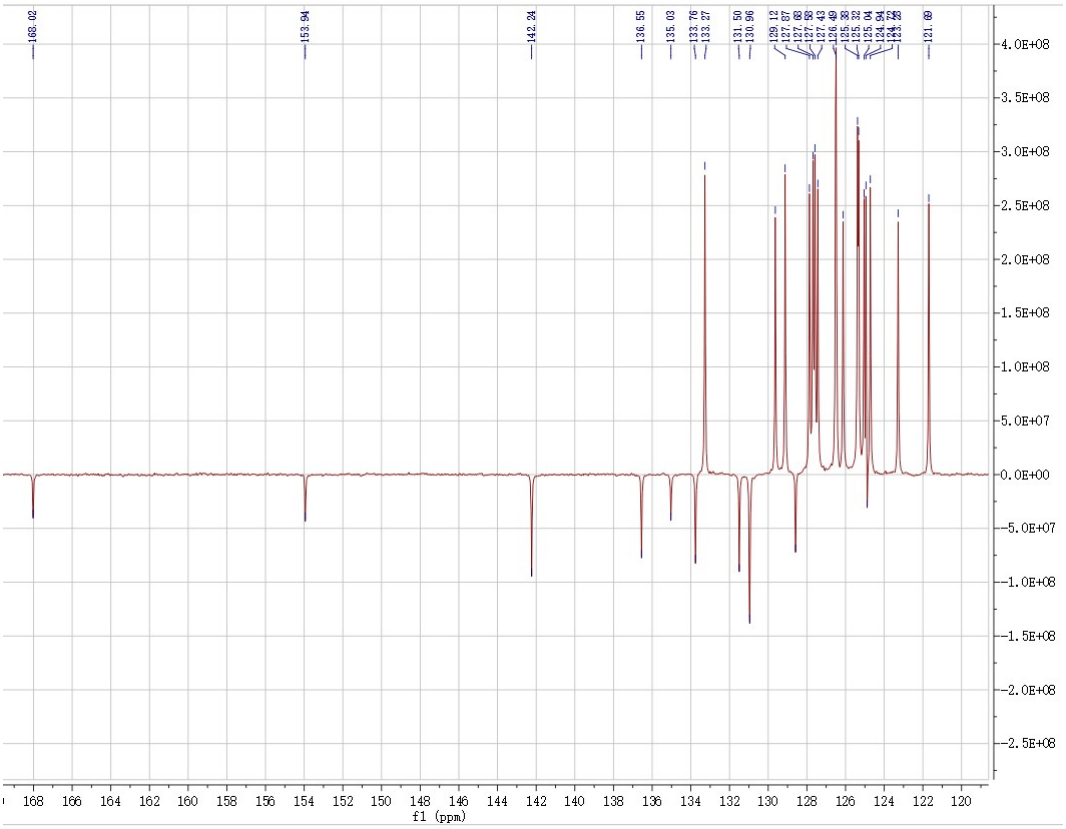

Figure S18. ^{13}C NMR spectrum of **Py-*m*BZT** compound.

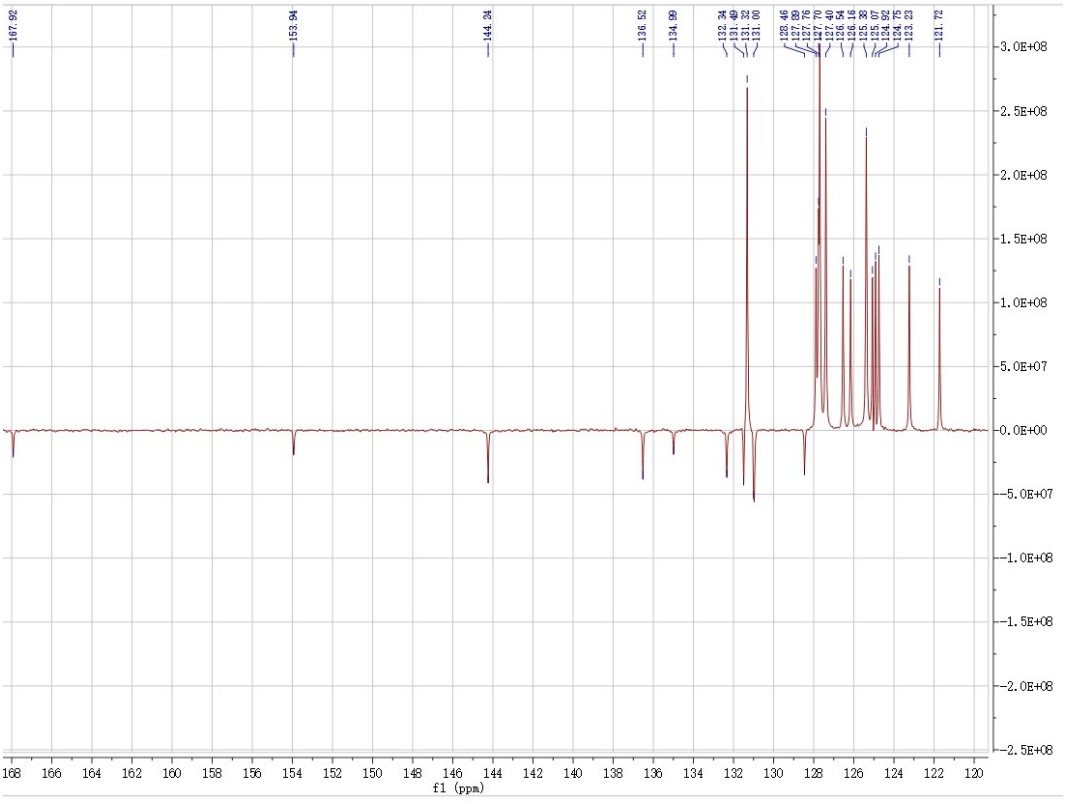

Figure S19. ^{13}C NMR spectrum of **Py-*p*BZT** compound.

SIV References

[1] M. J. Frisch, G. W. Trucks, H. B. Schlegel, G. E. Scuseria, M. A. Robb, J. R. Cheeseman, G. Scalmani, V. Barone, B. Mennucci, G. A. Petersson, H. Nakatsuji, M. Caricato, X. Li, H. P. Hratchian, A. F. Izmaylov, J. Bloino, G. Zheng, J. L. Sonnenberg, M. Hada, M. Ehara, K. Toyota, R. Fukuda, J. Hasegawa, M. Ishida, T. Nakajima, Y. Honda, O. Kitao, H. Nakai, T. Vreven, J. A. Montgomery, Jr., J. E. Peralta, F. Ogliaro, M. Bearpark, J. J. Heyd, E. Brothers, K. N. Kudin, V. N. Staroverov, T. Keith, R. Kobayashi, J. Normand, K. Raghavachari, A. Rendell, J. C. Burant, S. S. Iyengar, J. Tomasi, M. Cossi, N. Rega, J. M. Millam, M. Klene, J. E. Knox, J. B. Cross, V. Bakken, C. Adamo, J. Jaramillo, R. Gomperts, R. E. Stratmann, O. Yazyev, A. J. Austin, R. Cammi, C. Pomelli, J. W. Ochterski, R. L. Martin, K. Morokuma, V. G. Zakrzewski, G. A. Voth, P. Salvador, J. J. Dannenberg, S. Dapprich, A. D. Daniels, O. Farkas, J. B. Foresman, J. V. Ortiz, J. Cioslowski, and D. J. Fox, *Gaussian 09*, *Revision D.01*, Gaussian, Inc., Wallingford CT, **2013**.

[2] T. Lu, F. Chen, Multiwfn: a multifunctional wavefunction analyzer. *J Comput. Chem*. **2012**, *33*, 580–592.

[3] T. Lu, Molclus program, Version 1.9.9.6, http://www.keinsci.com/research/molclus.html (accessed Aug. 28th, 2021).

[4] X. Zhang, S. Wang, Z. Fu, C. Wang, Z. Yang, Y. Gao, H. Liu, S.-T. Zhang, C. Gu and B. Yang, *Adv. Funct. Mater.* **2023**, *33*, 2301228.